Title

A multi-modal scanning system to digitize CBRNE emergency response scenes

ISBN

9781665456807

Authors

Salathe, Marco
Quiter, Brian J
Bandstra, Mark S
et al.

Publication Date

2022-11-10

DOI

10.1109/ssrr56537.2022.10018826

Peer reviewed

A multi-modal scanning system to digitize CBRNE emergency response scenes

Marco Salathe[1], Brian J. Quiter[1], Mark S. Bandstra[1], Xin Chen[1], Victor Negut[1], Micah Folsom[1], Gunther H. Weber[2], Christopher Greulich[3], Mathew Swinney[3], Nicholas Prins[3], Daniel E. Archer[3]

***Abstract*— A handheld system developed to digitize a contextual understanding of the scene at a chemical, biological, radiological, nuclear and/or explosives (CBRNE) events is described. The system uses LiDAR and cameras to create a colorized 3D model of the environment, which helps domain experts that are supporting responders in the field. To generate the digitized model, a responder scans any suspicious objects and the surroundings by carrying the system through the scene. The scanning system provides a real-time user interface to inform the user about scanning progress and to indicate any areas that may have been missed either by the LiDAR sensors or the cameras. Currently, the collected data are post-processed on a different device, building a colorized triangular mesh of the encountered scene, with the intention of moving this pipeline to the scanner at a later point. The mesh is sufficiently compressed to be sent over a reduced bandwidth connection to a remote analyst. Furthermore, the system tracks fiducial markers attached to diagnostic equipment that is placed around the suspicious object. The resulting tracking information can be transmitted to remote analysts to further facilitate their supporting efforts. The paper will discuss the system's design, software components, the user interface used for scanning a scene, the necessary procedures for calibration of the sensors, and the processing steps of the resulting data. The discussion will close by evaluating the system's performance on 11 scenes.**

I. Introduction

There are scenarios where chemical, biological, radiological, nuclear and/or explosives (CBRNE)-trained first responders, arriving at a scene, are remotely supported by expert analysts. These analysts are typically experts in relevant fields and in the analysis of data generated by onsite diagnostics equipment. If these analysts were able to quickly obtain a realistic model of the scene and associated measurement activities, it would greatly facilitate their understanding of the context of measurements occurring at the scene and could facilitate communications with onsite personnel. This work is focusing on emergency situations involving radiological and/or nuclear concerns, where a model of the scene could serve as input to physics-based simulation codes (e.g., based on Monte Carlo tools [1][2]). Models and physics-based simulations could also prove greatly beneficial in understanding the measurements performed around the object that triggered the emergency response. Herein, we will refer to such an object as an item of primary concern (IPC).

Usage of systems with 3D scanning abilities so far has been spearheaded by criminal forensics using stationary systems [3]. Using LiDAR-based mapping for enhanced situational awareness of on-site CBRNE operators has also been focused on during development and deployment of robotic systems [4], [5], [6], [7], [8]. Reconstructions of scanner data have been investigated to support disaster management [9]. Additionally, various backpack-based and handheld systems have been proposed for use in indoor modeling [10], [11]. Similar systems have been utilized for radiation detection and imaging [12], [13]. To our knowledge use of 3D scanners to enhance situational awareness of remote experts has not been considered in the scientific discourse.

In light of these observations, a team of scientists at Lawrence Berkeley National Laboratory (LBNL) and Oak Ridge National Laboratory (ORNL) undertook the Semi-automated Scenes for Diagnostics (SaS4D) project to create a prototype handheld scanning system and corresponding processing algorithms to rapidly generate three-dimensional (3D) models of scenes that are: several 10's of MB in size, have visual labeling, and can be used to formulate watertight geometric models. The scanning task is performed with a portable system, carried through the scene by an onsite first responder. The scanning system addresses both the limited coverage that is typical of static scanning and helps address the complexities arising from autonomous navigation or remote operation necessary for unmanned vehicles. This solution does not directly address risks to first responders due to exposure to dangerous materials, chemicals, radiation, and explosive forces, but these risks could be reduced through the use of remotely operated robotic systems.

The SaS4D system incorporates software to detect fiducial markers placed on detection devices in the image stream from the camera. These markers can uniquely identify each item of equipment, simplifying the accounting of these devices on site and the communication about their placement around the IPC to remote analysts.

The design of the system, its user interface (UI), the analysis software, and some example data are summarized in this paper.

*This work was performed under the auspices of the US Department of Energy by Lawrence Berkeley National Laboratory under Contract DE-AC02-05CH11231. The project was funded by the US Department of Energy, National Nuclear Security Administration, Office of Defense Nuclear Nonproliferation Research and Development (DNN R&D).

[1] M. Salathe, M. S. Bandstra, B. J. Quiter, X. Chen, V. Negut and M. Folsom are with the Applied Nuclear Physics Program at Lawrence Berkeley National Laboratory, One Cyclotron Road, Berkeley, CA 94720, USA.

[2] G. Weber is with the Machine Learning and Analytics group within the Computer Science Research Division at Lawrence Berkeley National Laboratory.

[3] C. Greulich, M. Swinney, D. Archer, N. Prins are with the Oak Ridge National Laboratory, P.O. Box 2008, Oak Ridge, TN 37831, USA.

Email: msalathe@lbl.gov.

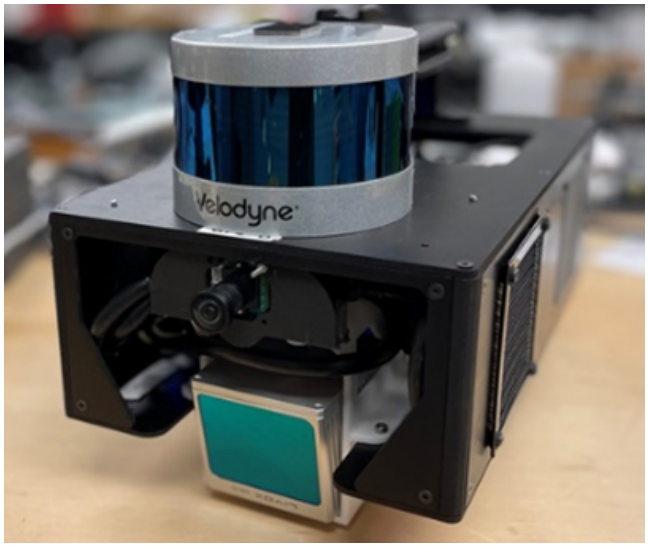

Fig. 1. Photo of the SaS4D handheld scanning system.

II. System overview

The SaS4D system (see Figure 1) is a hand-portable sensor system that has been designed as a scanner and tracker for emergency response CBRNE missions. Presently, the system is capable of rendering a realistic model of a scanned geometry in real-time, but performs additional post-processing in order to formulate better-fidelity models that are intended to be transmitted to off-site analysts through limited-bandwidth telecommunications.

Including batteries, the SaS4D scanner weighs about 4 kg and features the following sensors: a Velodyne Puck LITE 16 (VLP-16) LiDAR [14], a Livox Mid-70 LiDAR [15], a See3CAM_CU81 RGB camera [16] and a VectorNav VN200 Inertial Navigation System [17]. Additionally, it contains a NUC 11 computer with Intel 4 core (8 thread) i7 CPU and an integrated GPU [18]. The NUC's WiFi antennae are integrated into the enclosure housing, providing good signal strength in all directions. Ports to connect external hard drives for transferring recorded data are easily accessible on the back of the system. The system can be powered with one or two batteries or using external wall-power. The two-battery system gives users hot-swap capabilities; either battery can be removed and replaced with a new battery without needing to power down the system in the process. This means that field operation need not be interrupted during long campaigns. The system can run about 2.5 hours on two batteries while performing typical emergency response activities. A 90+% efficient power distribution units deliver both 16 V and 5 V outputs to provide power to the onboard sensors and computer. The handle features a camera cold shoe which can accept a variety of mountable devices such as external lighting or a mount to hold a tablet computer to render the user interface served by the NUC computer.

III. Software

All software components are deployed in individual Docker containers [19]. The containers are pre-built and

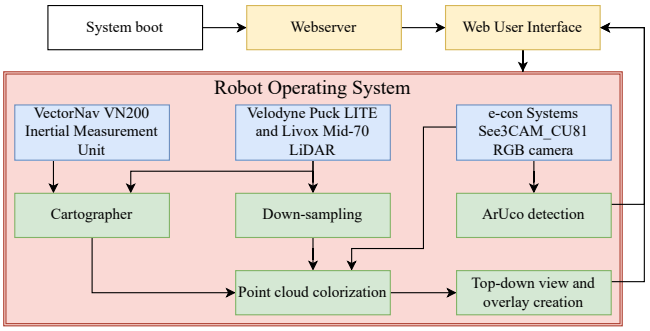

Fig. 2. A flow diagram of the sensor and software components.

stored in an online registry, which enables fast installation of the software stack on the SaS4D onboard computer and assures stable operation, without being affected by unwanted or breaking OS upgrades. Docker compose [19] is leveraged to orchestrate execution of the various Docker container that are required for operation of the system. The sensor drivers and data processing and recording units are based on the Robot Operating System (ROS) [20] node infrastructure and leverage the ROS message structure for communication. ROS is also used to save all sensor outputs to a file.

An overview of the data flow on the system, from sensors to processing units, is shown in Figure 2. The LiDAR sensors output data at 75 Hz as a collection of x, y, z coordinates relative to the sensor position – commonly referred to as point clouds. Cartographer [21], a real-time simultaneous localization and mapping (SLAM) framework, leverages the point clouds from the two LiDARs and the inertial measurement unit's linear acceleration and rotational velocity data to predict the systems location and orientation (Pose) at any point in time during a measurement.

The two point cloud data are combined and randomly down-sampled to about 5%. This is necessary to not exceed the NUC's computing power and assure real-time operation. The remaining points are projected to the camera's image plane, using the camera intrinsic and the extrinsic transformation between the physical Poses of the LiDARs and the camera. The camera operates at 20 Hz; the image closest in time to a given set of points is used to map a RGB color to each point. This is done by assigning the RGB value of a given pixel to all the points that were projected into the area covered by that pixel. Points outside the image are marked as (0, 0, 0) and thus recognizable in later processing steps.

By leveraging the Pose of the system as predicted by the SLAM algorithm, the colorized point cloud is assembled into a 3D voxel grid. The assembled voxel grid is reduced to a two-dimensional image in the form of an X-ray-like floor plan of the scanned area (see Figure 3), with walls and structures being represented by darker colors. During voxelization, the program keeps track of the fraction of LiDAR points in each voxel that received a color assignment during camera projection in the point cloud colorization step. This information is added as a red-transparent overlay over the floor plan to indicate areas which have not been seen by

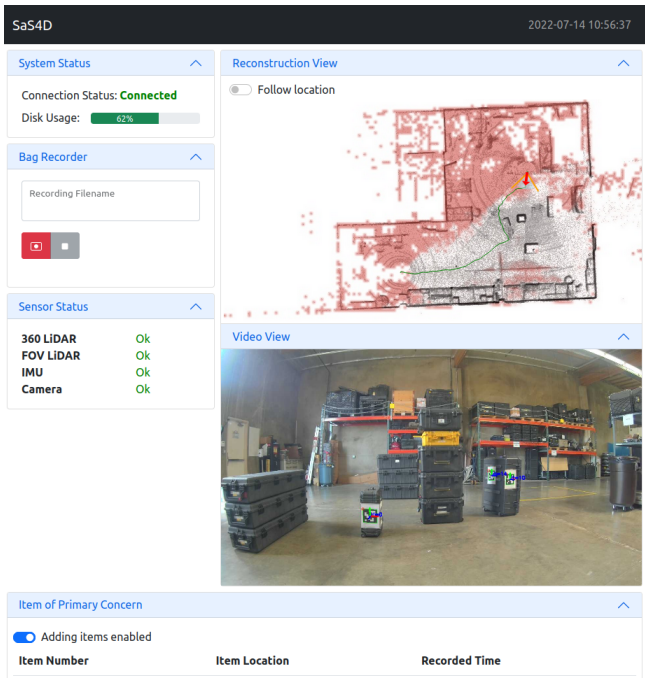

Fig. 3. The web-based user interface enables one to control and monitor the system.

the camera so far. The transparency is defined with a logic function based on the occupancy fraction. Figure 4 provides an example of how the visualization of camera coverage evolves as a scan progresses.

The camera images are down-sampled to about 5 Hz and any visible ArUco markers [22] in these images are localized and identified. The location, timestamp and identifier of every detected marker is transformed into the reference frame of the SLAM map and stored in a JavaScript Object Notation (JSON) file on disk. This file can then be sent, together with the finalized map to a remote team.

The system serves a web page at a dedicated address to function as a user interface (UI). The page can be accessed with an iPad, phone or computer on the same network. A screen shot of the user interface is shown in Figure 3. It has a pane that shows the floor plan with the progress overlay created by the data pipeline, a pane displaying the camera feed with ArUco markers overlaid, a dialogue to start and stop a measurement, annotate a measurement with a note and to drop a pin on the floor plan to mark locations of interest (which may be the IPC). All these data are displayed and updated in real-time to aid the user in the scanning process and to assess the quality of the already recorded data.

IV. Design Consideration

The choice to use two different LiDARs on the system was guided by the idea of the system being operated in two distinct modes. The first mode is 'scanning', where the system is carried through a scene, trying to create an external model of the dimensions of the IPC and nearby structures with great detail and sufficient camera coverage to potentially enable material identification. The second mode is 'tracking',

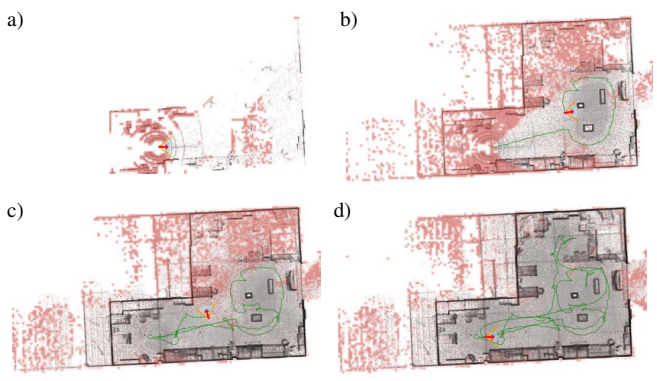

Fig. 4. Four views of the top-down projection of the point-cloud and camera-based colorization view in the SaS4D real-time user interface. As the scan progresses (from a to d), the detail rendered in the black-and-white point cloud projection increases. Similarly, the amount of area that is 'uncovered' by the camera changes significantly.

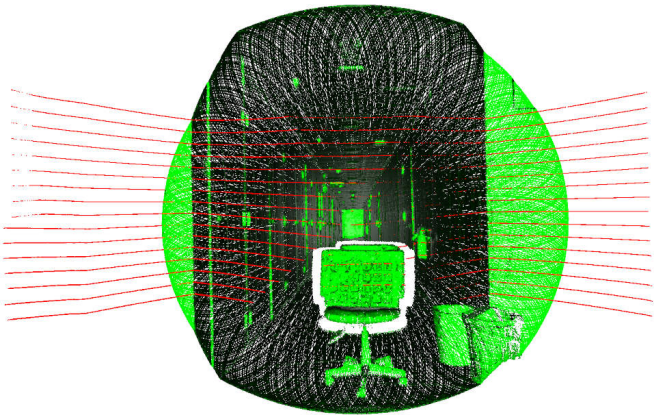

Fig. 5. The result of co-registration between the VLP-16 (red) and the Mid-70 (green) in a 40-m-long hallway with an ArUco marker board being held upright by an office chair at a distance of approximately 2 m. The dark shading of the green and red points indicate the normal angle relative to the viewing perspective, with no shading at 0° to black at 90°.

where the system is placed to statically monitor movements around the scene. The VLP-16 with its 360° field of view has proven very robust in providing the necessary coverage to reliably perform SLAM with centimeter fidelity. The ability of the VLP-16 to sense areas that have not yet been observed by the camera enables coupling with the UI to guide the user to ensure better camera coverage. The Mid-70, has a limited, circular field of view of 70° opening angle, that overlaps the field of view of the camera. It uses a variable scanning pattern, so that within a second more than 90% of the field of view are covered, with higher density towards the center of the field of view. Thanks to this dense coverage the LiDAR point cloud and camera images can be merged for various tracking tasks in 3D space, even when the system is static. The two LiDAR scanning patterns are visualized in Figure 5.

The selection of the See3CAM_CU81 camera has been governed by its observed performance on a portable system in low light conditions. The camera features a dynamic range of up to 140 dB, which assures that it can capture images with a short exposure even in back-lit situations.

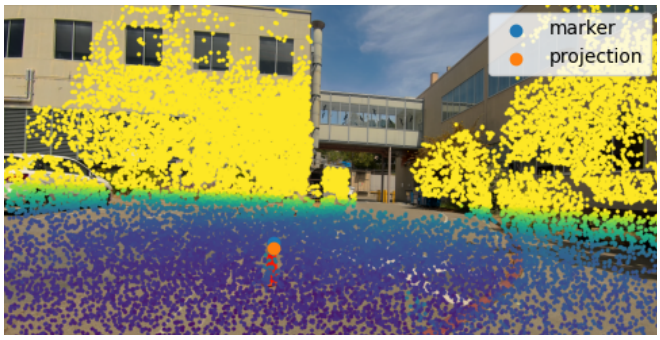

Fig. 6. Example of a point cloud overlaid on an image, with the point cloud-derived position of the cone tip marked in orange and the image-derived location marked in blue. The distance between the two is minimized in about 50 images for extrinsics and timing estimation.

This is particularly important to get sharp images during the scanning phase, where the system often is moved across surfaces at relatively high rotational speed. The 4k resolution of the camera, coupled with a custom lens of about 70° horizontal field of view enables the tracking of ArUco markers over large distances. The field of view of the camera also is similar to the one of the Mid-70 LiDAR. The camera, operating over USB 3.1 Gen 1, is able to deliver 15 Hz at 4K resolution and 30 Hz at a lower resolution.

V. Calibration

The extrinsic transformation between the two LiDARs was extracted from a static measurement of a 40-meter-long hallway by applying the iterative closest point algorithm implemented in Open3D [23] to the two data streams (see Figure 5). The intrinsics between the camera and the LiDARs were estimated by manually marking a cone tip in the point cloud resulting from SLAM and about 50 images and using a least-square minimization procedure to get the Pose difference and the time delay of the camera (see Figure 6). The transformation between the IMU and the other sensors was derived from CAD drawing of the system. The camera intrinsic and lens distortions were measured with a classical checkerboard calibration procedure.

VI. Post-processing

The goal is to execute all processing steps on the system itself. For now, however, the final data products are generated offline on a separate computer. It takes about 15 minutes to run the full offline pipeline for a 5-minute collection, from raw sensor data recorded with ROS to the final mesh of the scene, or about 3 times slower than real-time.

The first step in the offline pipeline is to re-run Cartographer with higher fidelity settings to create a file containing the system's trajectory through the scene. Next, a colorized point cloud map is created that has normal vectors estimated for each point. Images were filtered from 20 Hz to 5 Hz by selecting the image with the lowest Laplacian variance [24] to reduce the impact of image blur. Colorization is accomplished by first projecting each set of points (collected during a period of 75 Hz) to the surviving camera image captured nearest in time and assigning RGB values by the pixel associated with those LiDAR points. The trajectory from SLAM has been used to correct the difference in Pose between the recording time of the camera image and the point cloud. The Cartographer trajectory then is used to project the points measured at each location into space. A total of 48 point sets are aggregated and the normals are calculated on the aggregated set with a k-d tree based algorithm [23] and orientated toward the mean camera location during that 0.64-second period of aggregation. The resulting point cloud is stored to a PLY file. The data size at this point is about 700 MB per recorded minute and is thus too large to be easily transferred to offsite analysts. A more compact representation, that doesn't limit the interpretability of a scene, is a triangular mesh. The mesh is calculated by using a Poisson surface reconstruction algorithm [23] and the 7% quantile of points with the lowest density is removed. The resulting mesh is smoothed and reduced with quadric decimation to about 1 million vertices, again using techniques from [23]. The resulting mesh is about 80 MB which is significantly more readily transmitted.

VII. Evaluation

The system was used to capture three outdoor and eight indoor scenes. Each capture took about 5 minutes to collect and a selection of the resulting 80 MB meshes is shown in Figure 7. No issues were discovered while operating the system, but a few limitations were observed during post-processing. SLAM worked better in large spaces; SLAM requires the return distance of points to be above a lower threshold and can get deprived of points in confined spaces. This results in a slightly blurred point cloud and lumpy mesh surfaces. The presence of windows and other transparent materials causes laser pulses to be partially reflected, which produces mirror image of the scene on the other side of the window or vague boundaries along the transparent surfaces. Normal extraction in areas with large amounts of clutter is less reliable. This affects the quality of Poisson reconstruction and results in irregular surfaces.

An important part of the presented workflow is the ability to produce a compressed mesh that still captures shapes in the scene with high fidelity. Figure 8 shows the median distance between the points in the original point cloud and the nearest surface of the mesh after quadric decimation. Poisson reconstruction itself reduces the number of vertices in the mesh limiting the mesh fidelity of large scenes to about 3 cm and close to 1 cm for small scenes. Quadric decimation retains mesh fidelity well, only below 10^5 vertices the quality of the mesh starts to degrade considerably. The 80 MB meshes displayed in Figure 7 are about a factor of 10 above that limit so further compression is possible if necessary. The presented fidelity number does not describe the colorization aspects of the mesh, where having more points is definitely important but hard to quantify.

The tracking performance of ArUco markers was systematically evaluated by analyzing the board on the chair in Figure 5 with both LiDAR (for ground truth) and camera

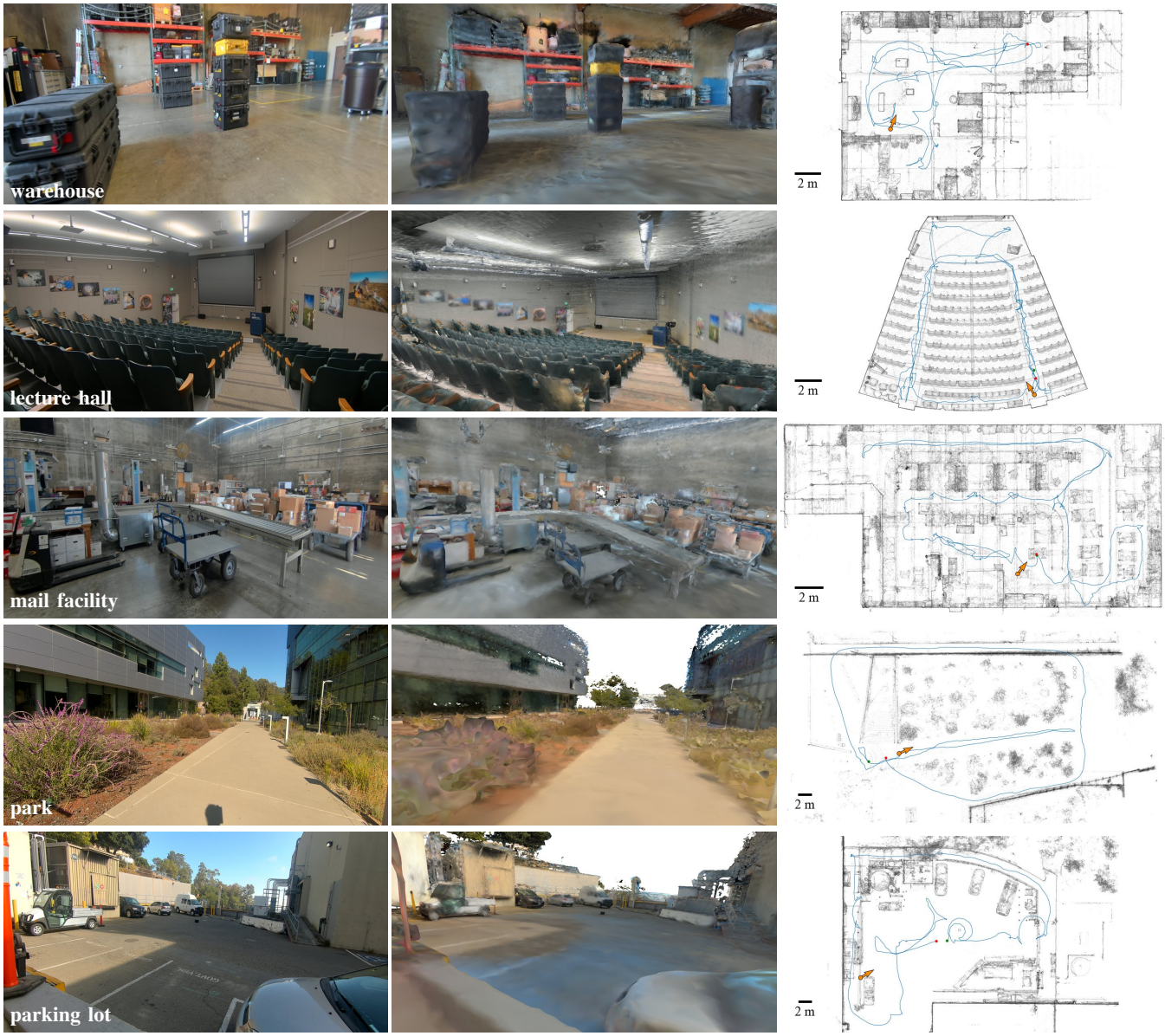

Fig. 7. A comparison between images recorded with the system (left) and the same view in the mesh (center).The white portions in the mesh are surfaces not measured by the LiDARs. On the right a x-ray top-down view of the scene is shown. Dark area indicate a lot of structures. The path travelled by the system is indicated in blue, the camera location and view directions (of the view in the other two panels) is represented with a orange dot and arrows.

images at different distances. It was found that at 3 meters, the 2-inch markers could reliably be detected with 3 cm accuracy. This number increases to about 10 cm accuracy at 8 m. Beyond that distance, not all 12 markers on the boards are consistently detected before losing all detection ability around the 10 meter mark. The orientation accuracy is about 10° for distances of less than 8 meters.

VIII. Conclusion

A system was designed and built to be used by a CBRNE first response team, with a focus on nuclear and radiological incidents. The system is handheld and allows one to create a 3D representation of an item of primary concern (IPC) and its surroundings that then can be sent over limited-bandwidth connections to offsite experts. The colorized mesh provides these experts with important contextual information and reduces the complexity of describing a scene verbally or with a limited number of photographs. The system is designed to be simple in its usage as a scene scanner and comes with a web-based user interface that informs the user about progress and data quality and allows one to annotate both through note-taking and spatially labeling areas of interest. The simplicity of the system and its usage is important for adoption of the system in field deployment missions with limited additional training needs.

Tracking of equipment is achieved with ArUco markers that are affixed to equipment surfaces and enable unique identification and localization of the various detection systems. Such unique identification can be coupled to equipment tracking and calibration databases. Tracking data can addi-

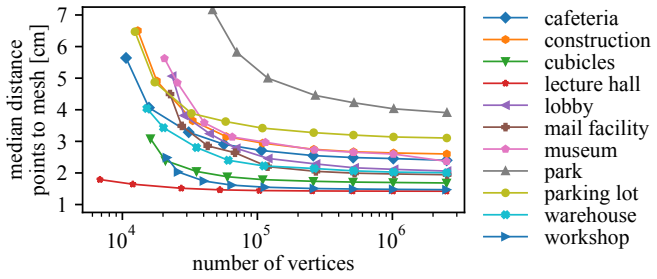

Fig. 8. A metric measuring the fidelity of the final mesh compared to the initial point cloud as a function of compression through quadric decimation.

tionally be transmitted to analysts to automate the documentation of diagnostic positioning and timing, which can further be used to automate aspects of formulation of physics-based simulations of the scene.

Subsequent to the initial scanning, the same handheld scanner has been designed to function as a passive recording device that locates the time and position of diagnostic measurement equipment within the scene over the course of the response action. Such a modality has been previously discussed in [25] and could inform the remote team about activities and changes near the IPC after the initial scan.

The transmitted mesh can be used as a basis to create models for physics-based simulations and thus help better understand diagnostic measurements. The process can be aided with modern computer vision tools, such as semantic segmentation, to assign distinct labels to volumes in the mesh and enable inference of material properties. These tools are actively being developed within the project and will be run on an upgraded compute platform (Jetson AGX Orin [26]) being installed and tested at present on the system.

Other upgrades will encompass moving the data processing pipeline, currently run offline on a separate device, onto the system itself. Last, but not least, the goal will be to enable dedicated scanning and tracking modalities and automatic switching between these modes based on inertial measurement unit data.

The lightweight system takes advantage of existing state-of-the-art sensor technologies and algorithms. It combines them in a unique and robust way to address existing needs of emergency response operations. This approach permitted a first demonstration with end users in early June 2022, where they could test and interact with the system directly. The direct feedback provided during the demonstration will guide further efforts in developing the system and hopefully bring useful modern computer vision techniques to the field within the foreseeable future.

References

[1] C. J. Werner, *MCNP6.2 Release Notes - report LA-UR-18-20808*, Los Alamos National Laboratory, 2018. [Online]. Available: https://laws.lanl.gov/vhosts/mcnp.lanl.gov/index.shtml

[2] S. Agostinelli *et al.*, "Geant4—a simulation toolkit," *Nuclear Instruments and Methods in Physics Research Section A: Accelerators, Spectrometers, Detectors and Associated Equipment*, vol. 506, no. 3, pp. 250–303, 2003.

[3] J. Morgan and G. LaPorte, "A Landscape Study of 3D Crime Scene Scanning Devices," The Forensic Technology Center of Excellence, Research Triangle Institute International, Tech. Rep., 2018. [Online]. Available: https://forensiccoe.org/private/5dd6ad2d0ffeb

[4] T. Röhling *et al.*, "CBRNE hazard detection with an unmanned vehicle," in *2009 IEEE International Workshop on Safety, Security & Rescue Robotics (SSRR 2009)*, 2009, pp. 1–5.

[5] P. Jasiobedzki *et al.*, "Increasing situation awareness of the CBRNE robot operators," in *Sensors, and Command, Control, Communications, and Intelligence (C3I) Technologies for Homeland Security and Homeland Defense IX*, E. M. Carapezza, Ed., vol. 7666, International Society for Optics and Photonics. SPIE, 2010, pp. 113 – 120.

[6] F. E. Schneider *et al.*, "Unmanned multi-robot CBRNE reconnaissance with mobile manipulation system description and technical validation," in *Proceedings of the 13th International Carpathian Control Conference (ICCC)*, 2012, pp. 637–642.

[7] R. Guzman *et al.*, "RESCUER: Development of a Modular Chemical, Biological, Radiological, and Nuclear Robot for Intervention, Sampling, and Situation Awareness*," *Journal of Field Robotics*, vol. 33, no. 7, pp. 931–945, 2016.

[8] A. Czetina *et al.*, "Robot assisted analysis of suspicious objects in public spaces using CBRN sensors in combination with high-resolution LIDAR," in *2019 IEEE International Symposium on Safety, Security, and Rescue Robotics (SSRR)*, 2019, pp. 256–262.

[9] S. Nikoohemat *et al.*, "Indoor 3d reconstruction from point clouds for optimal routing in complex buildings to support disaster management," *Automation in Construction*, vol. 113, p. 103109, 2020.

[10] V. V. Lehtola *et al.*, "Comparison of the selected state-of-the-art 3d indoor scanning and point cloud generation methods," *Remote Sensing*, vol. 9, no. 8, 2017.

[11] S. Karam *et al.*, "Design, calibration, and evaluation of a backpack indoor mobile mapping system," *Remote Sensing*, vol. 11, no. 8, 2019.

[12] D. Hellfeld *et al.*, "Free-moving quantitative gamma-ray imaging," *Scientific Reports*, vol. 11, no. 1, 2021.

[13] L. Marques *et al.*, "State-of-the-art mobile radiation detection systems for different scenarios," *Sensors*, vol. 21, no. 4, 2021.

[14] *Puck LITE*, Velodyne Lidar, Inc., 5521 Hellyer Avenue, San Jose, CA 95138 USA. [Online]. Available: https://velodynelidar.com/products/puck-lite/

[15] *Mid-70*, Livox Technology Company Limited Co. Ltd., 40th Floor, Sunlight Tower,248 Queen's Road East, Wanchai, Hong Kong. [Online]. Available: https://www.livoxtech.com/mid-70

[16] *See3CAM_CU81*, e-con Systems, Inc., Suite 565, 2003 Gateway PI, San Jose, CA 95110. [Online]. Available: https://www.e-consystems.com/usb-cameras/ar0821-8mp-4k-hdr-camera.asp

[17] *VN-200*, VectorNav Technologies, LLC, 10501 Markison Road, Dallas, TX 75238 USA. [Online]. Available: https://www.vectornav.com/products/vn-200

[18] *NUC 11 Performance i7*, Simply NUC, 495 Round Rock West Drive, Round Rock, TX 78681. [Online]. Available: https://simplynuc.com/product/nuc11pahi7-full

[19] *Docker*, Docker, Inc., 3790 El Camino Real # 1052, Palo Alto, CA 94306. [Online]. Available: https://docs.docker.com

[20] *Robot Operating System (ROS)*, Open Source Robotics Foundation, Inc., 170 S. Whisman Road, Building D, Suite A, Mountain View, CA 94041 USA. [Online]. Available: https://wiki.ros.org/noetic

[21] W. Hess *et al.*, "Real-time loop closure in 2d lidar slam," in *2016 IEEE International Conference on Robotics and Automation (ICRA)*, 2016, pp. 1271–1278. [Online]. Available: https://github.com/cartographer-project/cartographer

[22] S. Garrido-Jurado *et al.*, "Automatic generation and detection of highly reliable fiducial markers under occlusion," *Pattern Recognition*, vol. 47, no. 6, pp. 2280–2292, 2014.

[23] Q.-Y. Zhou *et al.*, "Open3D: A modern library for 3D data processing," *arXiv:1801.09847*, 2018. [Online]. Available: www.open3d.org

[24] R. Bansal *et al.*, "Blur image detection using laplacian operator and open-cv," in *2016 International Conference System Modeling & Advancement in Research Trends (SMART)*, 2016, pp. 63–67.

[25] C. M. Humphrey and J. A. Adams, "Robotic tasks for chemical, biological, radiological, nuclear and explosive incident response," *Advanced Robotics*, vol. 23, no. 9, pp. 1217–1232, 2009.

[26] *Jetson AGX Orin*, Nvidia Corporation, 2788 San Tomas Expressway, Santa Clara, CA 95051. [Online]. Available: https://www.nvidia.com/en-us/autonomous-machines/embedded-systems/jetson-orin/